





Article

PLK1 phosphorylation of ZW10 guides accurate chromosome segregation in mitosis

Sm Faysal Bellah ¹, Fangyuan Xiong¹, Zhen Dou ^{1,2}, Fengrui Yang¹, Xing Liu ^{1,2}, Xuebiao Yao^{1,2,*}, Xinjiao Gao^{1,2,*}, and Liangyu Zhang ^{1,2,*}

¹ MOE Key Laboratory for Membraneless Organelles and Cellular Dynamics, Hefei National Research Center for Physical Sciences at the Microscale, University of Science and Technology of China School of Life Sciences, Hefei 230027, China

² Anhui Key Laboratory for Cellular Dynamics and Chemical Biology, Hefei 230027, China

* Correspondence to: Liangyu Zhang, E-mail: lyzhang0@mail.ustc.edu.cn; Xuebiao Yao, E-mail: yaoxb@ustc.edu.cn; Xinjiao Gao, E-mail: gaox@ustc.edu.cn

Edited by Yaming Jiu

Stable transmission of genetic information during cell division requires faithful chromosome segregation. Mounting evidence has demonstrated that polo-like kinase 1 (PLK1) dynamics at kinetochores control correct kinetochore–microtubule attachments and subsequent silencing of the spindle assembly checkpoint. However, the mechanisms underlying PLK1-mediated silencing of the spindle checkpoint remain elusive. Here, we identified a regulatory mechanism by which PLK1-elicited zeste white 10 (ZW10) phosphorylation regulates spindle checkpoint silencing in mitosis. ZW10 is a cognate substrate of PLK1, and the phosphorylation of ZW10 at Ser12 enables dynamic ZW10–Zwint1 interactions. Inhibition of ZW10 phosphorylation resulted in misaligned chromosomes, while persistent expression of phospho-mimicking ZW10 mutant caused premature anaphase, in which sister chromatids entangled as cells entered anaphase. These findings reveal the previously uncharacterized PLK1–ZW10 interaction through which dynamic phosphorylation of ZW10 fine-tunes accurate chromosome segregation in mitosis.

Keywords: ZW10, PLK1, kinetochore, mitosis, phosphorylation

Introduction

Faithful chromosome segregation requires proper bipolar attachment of sister chromatids to microtubules stemming from opposite spindle poles. Chromosome movements during mitosis are governed by the interaction of spindle microtubules with a specialized chromosome domain located within the centromere. Proper bi-orientation of chromosomes is essential for maintaining genomic integrity during mitosis (Cleveland et al., 2003; Liu et al., 2020). Several key mitotic kinases, such as polo-like kinase 1 (PLK1), Mps1, CDK1, and Aurora B kinase, are responsible for regulating the kinetochore–microtubule (KT–MT) attachment during mitosis. PLK1 is an important kinase that orchestrates this process and is involved in the regulation of centrosome maturation, mitotic entry, checkpoint recovery,

spindle assembly, sister chromatid separation, and even cytokinesis (Archambault and Glover, 2009; Zitouni et al., 2014). From the G2 phase to mitosis, PLK1 is localized at centrosomes. During mitosis, PLK1 accumulates at kinetochores from prophase to metaphase and is translocated to the midzone in anaphase (Golsteyn et al., 1995; Takaki et al., 2008). PLK1 is highly conserved among different species, with at least one PLK family member present from fungi to humans (Archambault and Glover, 2009; Zitouni et al., 2014). In vertebrate cells, PLK1 localizes to kinetochores during early mitosis and usually accumulates on unaligned chromosomes (Ahonen et al., 2005; Liu et al., 2012; Yu et al., 2020). During early mitosis, PLK1 stabilizes KT–MT attachments at kinetochores, whereas Aurora B destabilizes them (Lampson and Kapoor, 2005; Godek et al., 2015). Therefore, a tug of war between PLK1 and Aurora B kinase establishes a balance for the initial formation of stable KT–MT attachments. Previous studies showed that Aurora B kinase activity is high during prophase (Liu et al., 2009; Lampson and Cheeseman, 2011); therefore, high PLK1 activity is needed to balance the Aurora B activity. Inhibition or depletion of PLK1 leads to the arrest of cells in a prometaphase-like state, with unseparated centrosomes, monopolar spindles, and defects in KT–MT

Received September 3, 2023. Revised November 9, 2023. Accepted February 23, 2024.

© The Author(s) (2024). Published by Oxford University Press on behalf of *Journal of Molecular Cell Biology*, CEMCS, CAS.

This is an Open Access article distributed under the terms of the Creative Commons Attribution-NonCommercial License (<https://creativecommons.org/licenses/by-nc/4.0/>), which permits non-commercial re-use, distribution, and reproduction in any medium, provided the original work is properly cited. For commercial re-use, please contact journals.permissions@oup.com

attachment and chromosome alignment (Gimenez-Abian et al., 2004; Sumara et al., 2004; Hanisch et al., 2006; Lenart et al., 2007).

Zeste white 10 (ZW10) is a kinetochore protein, participates in mitotic checkpoint signaling and membrane trafficking between the endoplasmic reticulum (ER) and the Golgi, and serves to link dynactin and dynein to mitotic kinetochores. ZW10 exhibits dynamic subcellular localization during the cell division cycle. ZW10 binds to centromeres during prophase and anaphase (Williams et al., 1996). During interphase, ZW10 localizes to the cytoplasm and moves to the kinetochore as the cell enters mitosis. Interestingly, careful examination of the subcellular localization of ZW10 in interphase cells revealed its role in membrane trafficking between the Golgi and the ER via interacting with the SNARE complex involving syntaxin 18 (Hirose et al., 2004). The lack of a stable Bub1–Mad1/2 interaction in human cells could be due to the presence of the ROD–Zwilch–ZW10 (RZZ) complex, which is only present in complex eukaryotes and contributes to Mad1/2 kinetochore localization and checkpoint signaling (Basto et al., 2000; Buffin et al., 2005; Karess, 2005; Barisic and Geley, 2011). The RZZ complex has been proposed to be recruited to kinetochores via a direct interaction between ZW10 and the outer kinetochore protein Zwint1 (Wang et al., 2004; Kops et al., 2005). Zwint1 specifies the kinetochore association of ZW10 by interacting with its N-terminal domain. Suppression of Zwint1 synthesis by small interfering RNA (siRNA) abolishes the localization of ZW10 to the kinetochore. These Zwint1-suppressed cells display a chromosome bridge phenotype with sister chromatids interconnected. Importantly, the interaction between ZW10 and Zwint1 is required for the spindle checkpoint machinery to ensure faithful chromosome segregation in mitosis (Wang et al., 2004). However, whether there is a direct interaction between ZW10 and PLK1 and whether PLK1 plays a role in the regulation of ZW10 localization and function during the cell cycle still remain unclear.

In this study, we investigated how PLK1 mediates dynamic phosphorylation of ZW10 to ensure accurate chromosome segregation and chromatid separation.

Results

ZW10 is a novel interacting protein of PLK1

To study the molecular association of ZW10 with other accessory proteins in interphase and mitotic cells, we performed immunoprecipitation (IP) with ZW10 antibody (anti-ZW10 IP) to isolate ZW10-containing protein complexes, followed by mass spectrometric identification of tryptic peptides derived from the complexes (Fang et al., 2006; Yuan et al., 2007; Ding et al., 2010; Xu et al., 2021). Specifically, HeLa cells stably expressing green fluorescent protein (GFP)-tagged ZW10 were synchronized to different cell cycle stages, and PLK1 was found in ZW10 immunoprecipitates from mitotic but not interphase HeLa cells (Supplementary Table S1). Then, we performed anti-FLAG IP, followed by Coomassie Brilliant Blue (CBB) staining and western blotting, and validated the presence of PLK1 in FLAG immunoprecipitates from mitotic but not

asynchronized FLAG-ZW10-expressing HeLa cells (Figure 1A, lane 4). In addition, endogenous anti-ZW10 IP pulled down PLK1 from mitotic cell lysates (Figure 1B, lane 4), and a reciprocal co-IP assay confirmed the mutual interaction between ZW10 and PLK1 in HEK293T cells co-transfected with FLAG-PLK1 and GFP-ZW10 (Supplementary Figure S1A). Thus, we conclude that ZW10 forms a complex with PLK1 in mitotic cells.

PLK1 is a critical mitotic kinase that guides accurate KT–MT attachments (Yuan et al., 2007; Chu et al., 2011; Zhang et al., 2011). PLK1 plays pleiotropic roles during mitosis and is essential for mitotic division from the start until the end. PLK1 controls mitotic entry, centrosome separation and maturation, chromosome arm resolution, KT–MT attachment, spindle assembly checkpoint (SAC) silencing, and cytokinesis (Schmucker and Sumara, 2014; Xu et al., 2021). Our previous study revealed that ZW10 is located at the kinetochore in prometaphase (Wang et al., 2004). The biochemical association between ZW10 and PLK1 prompted us to examine whether ZW10 co-localizes with PLK1 to the kinetochore in HeLa cells during mitosis. As shown in Figure 1C (upper panel), ZW10 signal was readily apparent at the kinetochore, where it was superimposed on anti-centromere antibody (ACA) signal, in a prometaphase cell, indicating that ZW10 becomes localized to the centromere/kinetochore during early mitosis. Importantly, the co-distribution of ZW10 and ACA peaked in prometaphase cells, as the ZW10 signal at the kinetochore decreased in metaphase cells (Figure 1C and D), indicating dynamic localization of ZW10 to the kinetochore. Meanwhile, ZW10 co-localized with PLK1 in prometaphase cells, but both ZW10 and PLK1 signals at the kinetochore greatly declined as chromosomes aligned at the metaphase equator (Supplementary Figure S1B). Thus, we conclude that ZW10 complexes and co-distributes with PLK1 at the kinetochore during the early phase of mitosis.

Characterization of PLK1–ZW10 interactions

To delineate the specific binding interface between ZW10 and PLK1, we constructed deletion mutants of ZW10 (Figure 2A) and examined their localization and interactions with PLK1 in HeLa cells. ZW10, ROD, and Zwilch require each other for kinetochore localization (Scaerou et al., 2001; Williams et al., 2003) and form a complex known as the RZZ complex, which is recruited to kinetochores by Zwint1 (Wang et al., 2004). However, the structural determinant of ZW10 localization to the kinetochore and interaction with PLK1 remains elusive. Our previous biochemical studies indicated that Zwint1 interacts with the 80 N-terminal amino acids of ZW10 (Wang et al., 2004). As shown in Figure 2B, ZW10 N-terminal fragment (aa 1–470) localized to the kinetochore and co-distributed with PLK1, similar to full-length ZW10, in mitotic cells, indicating that its kinetochore localization depends on the N-terminal but not C-terminal region, consistent with our previous finding (Wang et al., 2004). Statistical analyses of immunofluorescence intensities of GFP-tagged ZW10 and the deletion mutants confirmed that the region containing the N-terminus is the determinant of ZW10 localization to the kinetochore (Figure 2C). We then performed

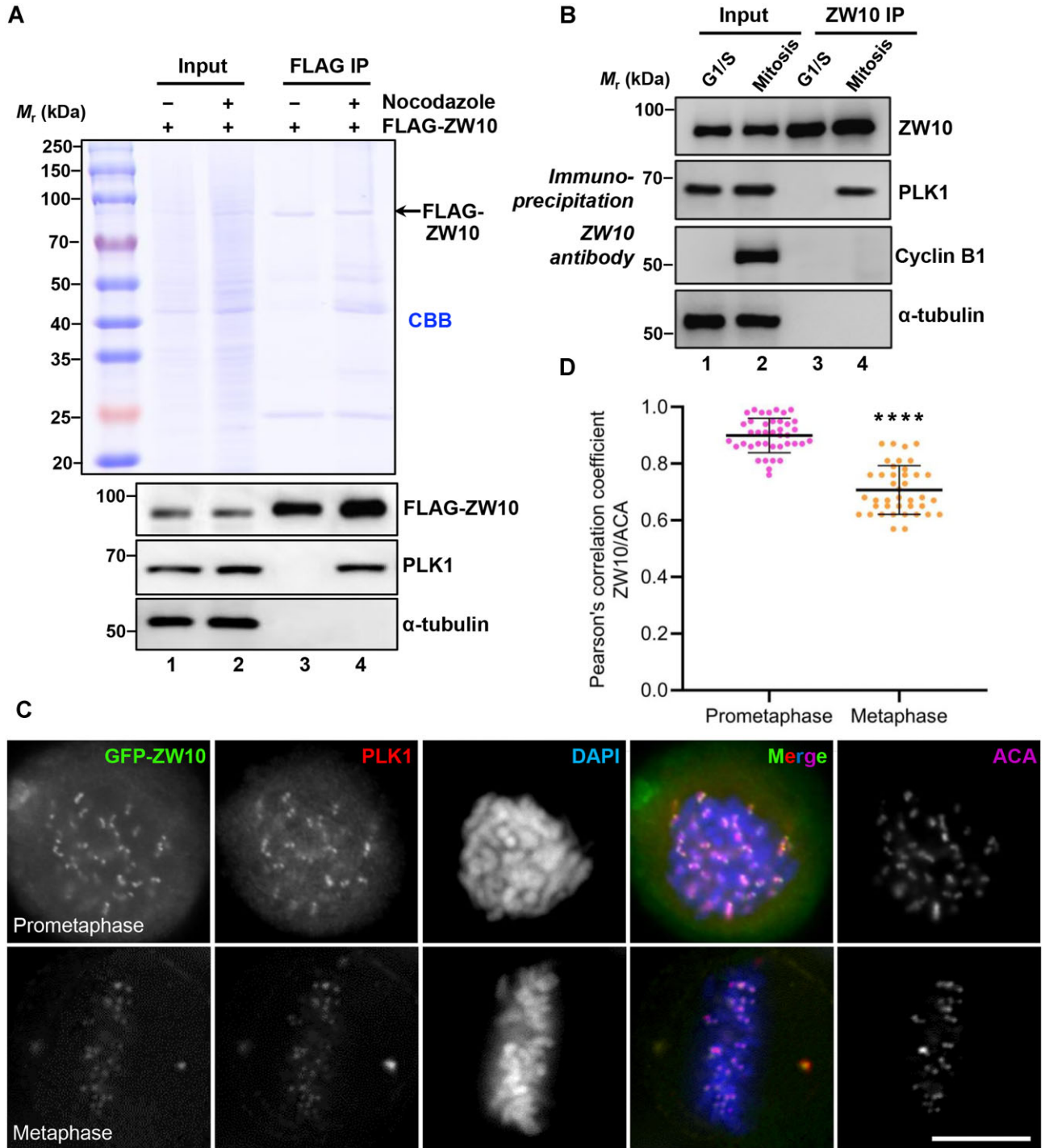


Figure 1 ZW10 is a novel interacting protein of PLK1. **(A)** Analyses of FLAG-ZW10 immunoprecipitates by CBB staining and western blotting. Anti-FLAG IP was performed with asynchronized or mitotic (100 ng/ml nocodazole, 18 h) FLAG-ZW10-expressing HeLa cells. Western blotting analyses confirmed the presence of PLK1 in the immunoprecipitates. **(B)** Endogenous IP assay. Endogenous ZW10 immunoprecipitates from interphase (G1/S, 2 mM thymidine for 17 h) or mitotic (100 ng/ml nocodazole for 16–18 h) HeLa cells were analyzed with antibodies against ZW10, PLK1, Cyclin B1, and α -tubulin. **(C)** Immunofluorescence staining of PLK1 and ACA in mitotic GFP-ZW10 stable HeLa Kyoto cells. GFP-ZW10 was visualized by direct GFP fluorescence, and DNA was stained with 4',6-diamidino-2-phenylindole (DAPI). The co-distribution of ZW10 with PLK1 was apparent at the centromere region in prometaphase and metaphase cells. Scale bar, 10 μ m. **(D)** Pearson's correlation coefficient values for co-localization of ZW10 and ACA at prometaphase and metaphase of GFP-ZW10 stable HeLa Kyoto cells. The average Pearson's correlation coefficients were calculated from 10 randomly selected kinetochores in every 40 prometaphase or metaphase cells from three independent experiments. **** $P < 0.0001$.

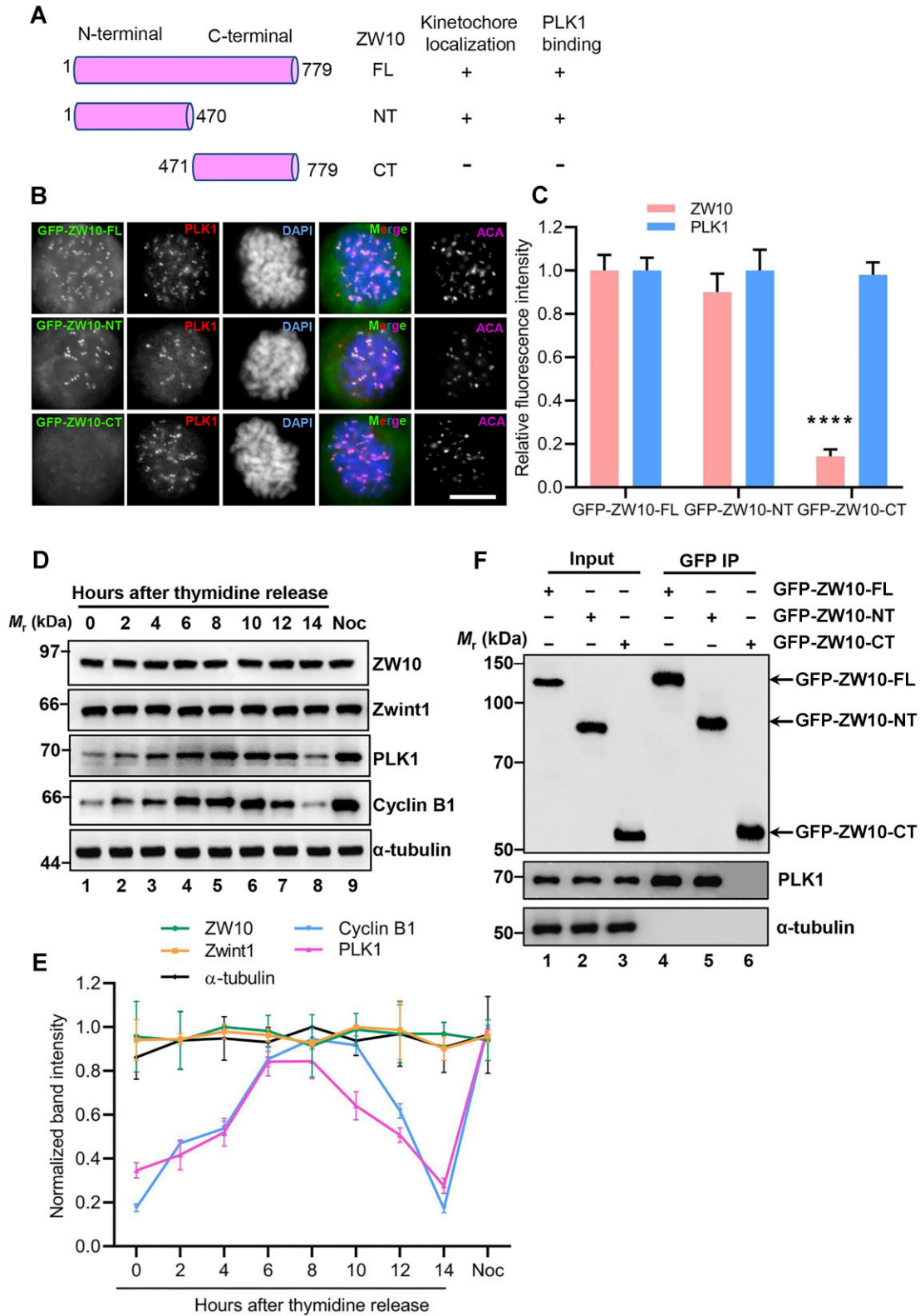


Figure 2 ZW10 interacts with PLK1 via the N-terminal domain. **(A)** Schematic representation of different ZW10 deletion mutants. +, positive; -, negative. FL, full-length, aa 1-779; NT, N-terminal, aa 1-470; CT, C-terminal, aa 471-779. **(B)** Immunofluorescence images showing the localization of transiently expressed GFP-ZW10-FL, GFP-ZW10-NT, and GFP-ZW10-CT in mitotic HeLa cells. At 24 h post-transfection, the cells were fixed and stained for PLK1, ACA, and DNA (DAPI). GFP-ZW10 and its truncations were visualized by direct GFP

live cell imaging of HeLa cells expressing GFP-tagged full-length or different fragments of ZW10. As predicted, full-length and N-terminal fragment (aa 1–470) of ZW10 localized to the kinetochore during mitosis (Supplementary Figure S2).

Next, we sought to examine the temporal dynamics of ZW10 and PLK1 protein expression during the cell cycle. For this purpose, we assessed the temporal profile of ZW10 levels from G1/S phase to mitosis relative to that of Cyclin B1, Zwint1, PLK1, and tubulin in synchronized HeLa cells by western blotting. Intriguingly, the ZW10 expression profile was rather constant during the cell cycle, different from that of Cyclin B1 and PLK1, which peaked during mitosis (Figure 2D; lanes 5 and 9). Thus, the protein level of ZW10 is relatively static throughout the cell cycle, while dynamic localization of ZW10 to the kinetochore is a function of mitotic progression (Figure 2E).

To determine the specific domain and contacts required for the ZW10–PLK1 interaction at the kinetochore, we carried out anti-GFP IP, followed by western blotting analysis. The results indicated that PLK1 was present in GFP immunoprecipitates from mitotic HeLa cells expressing full-length and N-terminal fragment of ZW10 but not those expressing C-terminal fragment of ZW10 (Figure 2F). The N-terminal region of ZW10 does not contain any Ser/Thr–Pro motif (data not shown), whose phosphorylation by CDK1 usually serves as a binding site for the Polo box of PLK1 (Elia et al., 2003a, b). Thus, the N-terminus of ZW10 likely complexes with PLK1 via a non-canonical mechanism.

ZW10 is a novel substrate of PLK1

The spatiotemporal localization and interaction profile of ZW10 with PLK1 in mitosis prompted us to investigate their binding interface and inter-relationship. To further confirm the physical interaction between these two proteins, we carried out a pull-down assay using bacterially expressed recombinant GST-ZW10 as an affinity matrix to absorb purified His-PLK1. As shown in Figure 3A, PLK1 bound to GST-ZW10 but not to the GST tag (lane 4 vs. lane 5). We next examined whether ZW10 localization to the kinetochore is a function of PLK1 kinase activity. As shown in Supplementary Figure S3A and B, ZW10 signal at the kinetochore was moderately weaker in cells treated with the PLK1 inhibitor BI-2536, suggesting that ZW10 kinetochore localization is regulated by PLK1 kinase activity. Several phosphorylation sites on endogenous ZW10 were identified by large-scale mass spectrometric analyses (PhosphoSitePlus) (Figure 3B; Supplementary Figure S3C). To identify the specific

PLK1-elicited phosphorylation sites on ZW10, we mutated Ser12 from the N-terminus and carried out an *in vitro* phosphorylation assay using recombinant wild-type (GST-ZW10-WT) and non-phosphorylatable mutant (GST-ZW10-S12A) ZW10 proteins (Figure 3C). Centromere protein U (CENP-U) was previously demonstrated to be a PLK1 substrate and thus used as a positive control (Hua et al., 2011; Singh et al., 2021). Phos-tag gel analysis showed that ZW10-WT was phosphorylated by PLK1 kinase, while the ZW10-S12A mutant was not (Figure 3C, top panel, lane 4 vs. lane 6). Thus, Ser12 is the main PLK1-elicited phosphorylation site on ZW10. Subsequently, we focused on this site to elucidate the functional significance of ZW10 phosphorylation mediated by PLK1 in mitosis.

Phosphorylation of ZW10 by PLK1 is essential for accurate chromosome segregation

We first characterized the phenotype associated with ZW10 suppression. As shown in Figure 4A, ZW10 siRNA efficiently suppressed ZW10 protein level at 48 h post-transfection, as judged by western blotting, while the level of PLK1 was not altered. Immunofluorescence imaging confirmed that ZW10 siRNA significantly reduced the relative fluorescence intensity of ZW10 to ACA (Supplementary Figure S4A and B). Live cell imaging with HeLa cells expressing mCherry-H2B showed that suppression of ZW10 resulted in chromosome segregation errors such as premature anaphase and chromatid bridges (Figure 4B). To ensure that the observed phenotypes were not due to off-target effects, a rescue experiment was carried out with HeLa cells expressing siRNA-resistant GFP-ZW10. As shown in Figure 4C, exogenously expressed siRNA-resistant GFP-ZW10 readily localized to the kinetochore soon after the cell entered mitosis (bottom panel; 5 min); the cell expressing siRNA-resistant GFP-ZW10 achieved metaphase alignment at 35 min when the signal of kinetochore ZW10 greatly declined and then progressed into anaphase at 45 min with equally segregated chromatids (similar to that observed in the siControl group). Statistical analyses of the data from three independent experiments indicated that siRNA-mediated ZW10 suppression resulted in chromosome misalignment and lagging chromosomes, which were rescued by the introduction of siRNA-resistant GFP-ZW10 (Figure 4D and E).

Next, we performed live cell imaging with HeLa cells expressing GFP-tubulin and mCherry-H2B. As predicted, normal cell division was observed in control siRNA-treated cells, while mitotic defects and microtubule disruption occurred in

Figure 2 (Continued) fluorescence. Scale bar, 10 μ m. (C) Quantification of ZW10 and PLK1 fluorescence intensities at the centromere/kinetochore. Note that the level of kinetochore-associated GFP-ZW10-CT is much lower than that of GFP-ZW10-FL and GFP-ZW10-NT. $n = 32$ mitotic cells from three independent experiments were surveyed for each condition. Data are presented as mean \pm SD; two-sided t -test; **** $P < 0.0001$. (D and E) Temporal expression profile of ZW10 during the cell cycle. Noc, 100 ng/ml nocodazole for 16–18 h. (D) Western blotting analyses of ZW10 in synchronized HeLa cells. Notably, the protein levels of ZW10 and Zwint1 are relatively stable, while those of PLK1 and Cyclin B1 change from interphase to mitosis. Tubulin was blotted as a loading control. (E) Quantification of relative protein levels of PLK1 and other proteins. The maximum average value of each protein throughout the cell cycle was set to 1. Data are presented as mean \pm SD from three independent experiments. (F) Analyses of GFP-ZW10 immunoprecipitates by western blotting. Anti-GFP IP was performed with mitotic (100 ng/ml nocodazole, 16–18 h) HeLa cells, and the immunoprecipitates were analyzed with antibodies against GFP, PLK1, and α -tubulin.

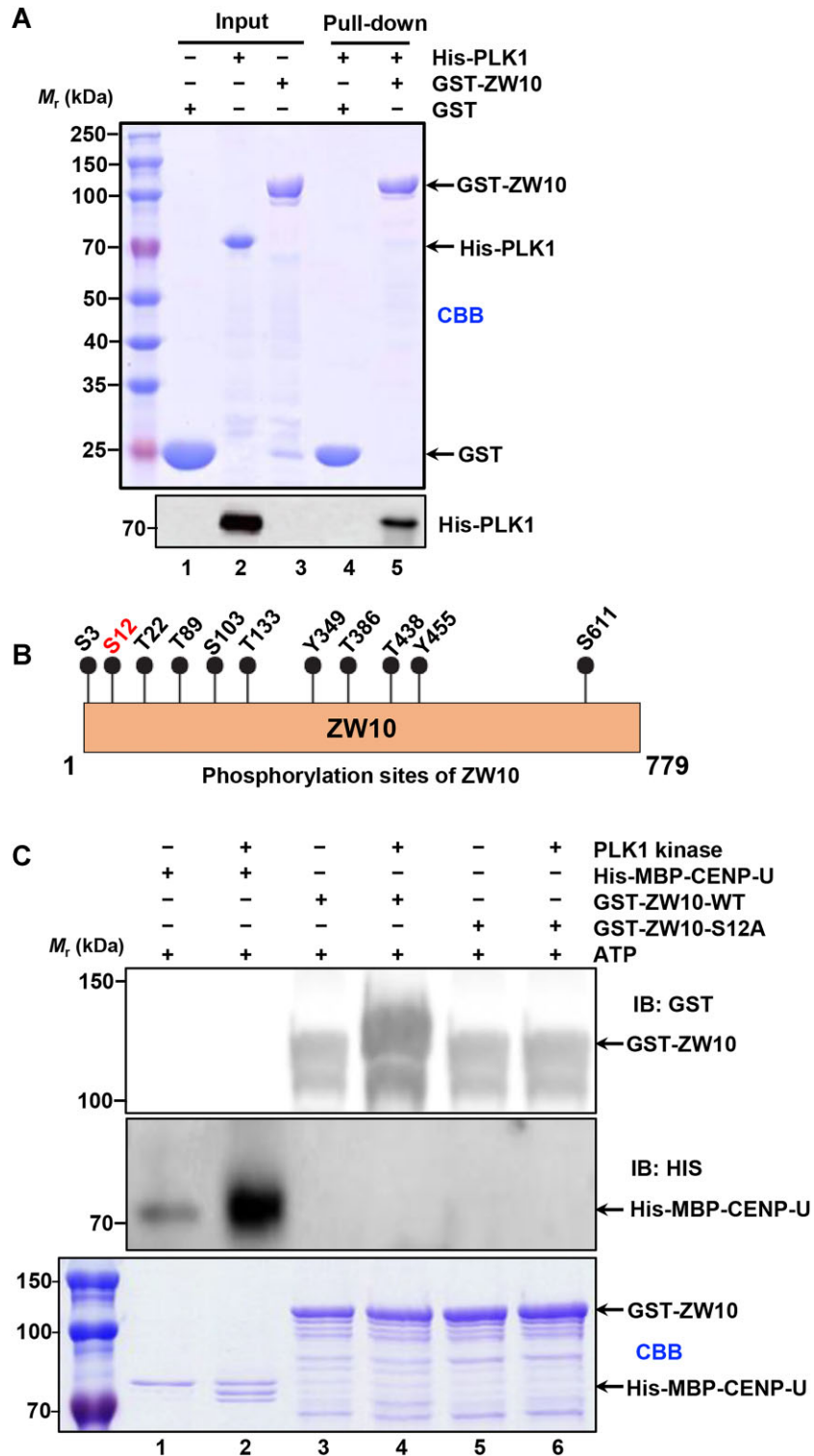


Figure 3 ZW10 is a novel substrate of PLK1. **(A)** *In vitro* pull-down of His-PLK1 by GST-ZW10 and analyses with CBB and western blotting. **(B)** Schematic showing the phosphorylation sites of endogenous ZW10 collected by PhosphoSitePlus. **(C)** *In vitro* phosphorylation assay and Phos-tag gel analysis showing that PLK1 phosphorylates ZW10 at Ser12. A phospho-shift of GST-ZW10 (GST-ZW10-WT but not GST-ZW10-S12A) by PLK1 (top panel). His-MBP-CENP-U was included as a positive control (middle panel). CBB staining of the gel (bottom panel). IB, immunoblotting.

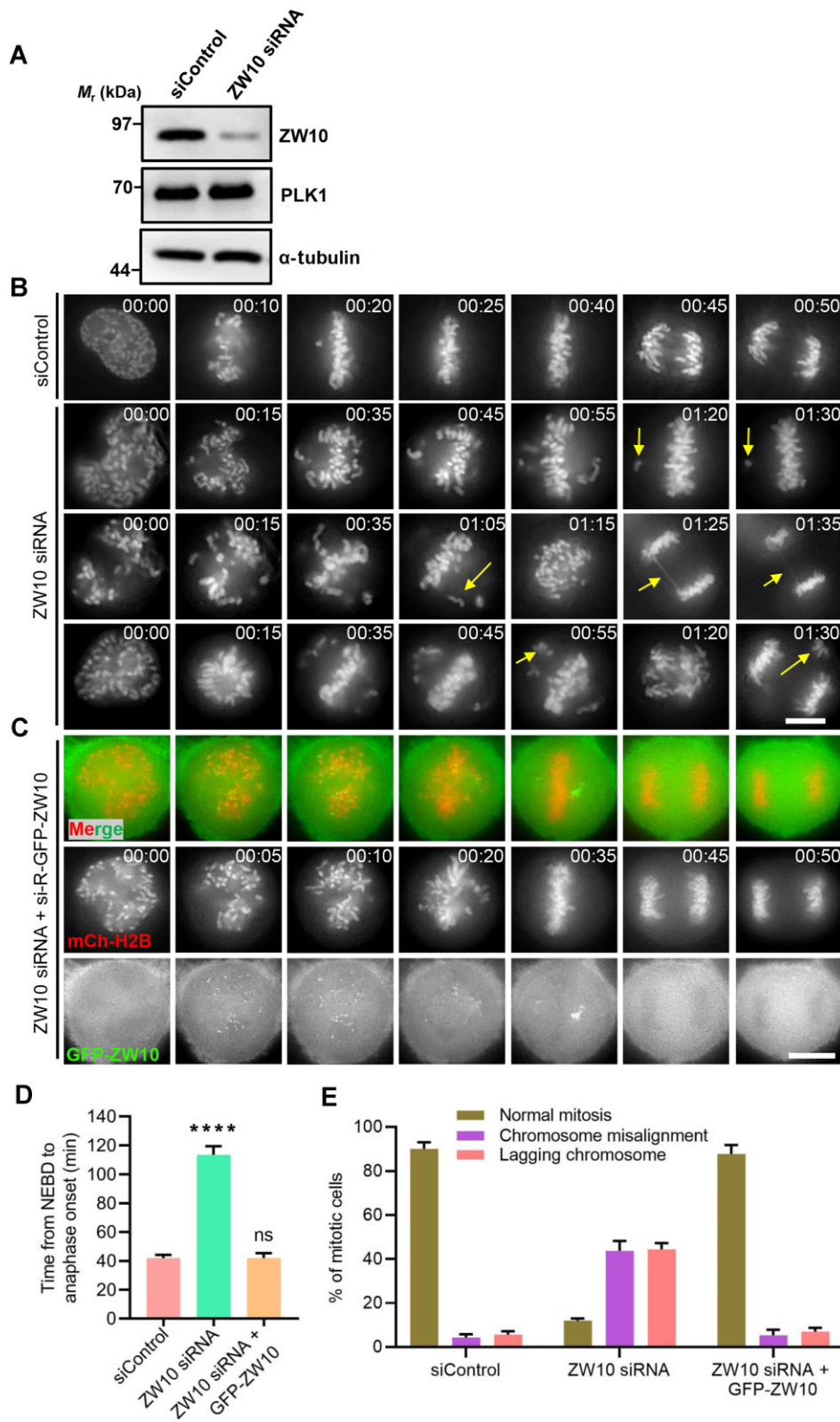


Figure 4 Knocking down ZW10 causes mitotic defects. **(A)** Characterization of the knockdown efficiency of ZW10 siRNA. Western blotting analysis of ZW10 protein levels at 48 h post-transfection with ZW10 siRNA. Tubulin was blotted as a loading control. **(B)** Suppression of ZW10 causes mitotic defects. HeLa cells were transfected with ZW10 siRNA along with mCherry-H2B as a marker of chromosomes. At 24 h post-transfection, the cells were synchronized for real-time imaging. The time is indicated in minutes. Scale bar, 10 μ m.

ZW10-deficient cells (Supplementary Figure S4C, top and middle panels). In particular, control siRNA-treated cells achieved metaphase at 20–30 min, while neither ZW10-depleted cells nor PLK1-depleted cells (Supplementary Figure S4E) exhibited normal metaphase, as judged by the presence of misaligned chromosomes, even at 90 min (Supplementary Figure S4C, middle and bottom panels). Statistical analyses confirmed that depletion of ZW10 or PLK1 caused severe mitotic defects, including chromosome alignment errors and lagging chromosomes (Supplementary Figure S4D). Proper KT–MT attachments are necessary for chromosome alignment and segregation during mitosis. They are mediated by the molecular motor dynein, CENP-E, and the KT–MT-binding complex NDC80. RZZ, which is essential for dynein recruitment via Spindly and plays a crucial role in the regulation of stable KT–MT attachments, is at the center of this coordination (Amin et al., 2018). Thus, we speculated that dynamic phosphorylation of ZW10 may be involved in correcting aberrant KT–MT attachments.

Then, we introduced GFP-tagged ZW10 proteins into HeLa cells depleted of endogenous ZW10. Western blotting analysis showed that the protein level of exogenously expressed GFP-ZW10 was comparable to that of endogenous ZW10 on average (Supplementary Figure S5C). Given that the transfection efficiency was ~40% (Supplementary Figure S5A and B), the expression level of exogenous GFP-ZW10 within each cell was estimated to be ~2.5-fold higher than that of endogenous ZW10. Live cell imaging of HeLa cells expressing mCherry-H2B demonstrated that expression of GFP-ZW10-WT supported accurate chromosome segregation in the absence or presence of endogenous ZW10, while expression of non-phosphorylatable GFP-ZW10-S12A resulted in a brief mitotic arrest and ~15 min delay in metaphase achievement after nuclear envelope breakdown (NEBD) (Figure 5A; Supplementary Figure S6A; top and middle panels). Surprisingly, phospho-mimicking GFP-ZW10-S12D failed to localize to the kinetochore, and persistent expression of GFP-ZW10-S12D resulted in abnormal anaphase with lagging chromosomes (Figure 5A; Supplementary Figure S6A; bottom panel). Statistical analyses of the data from three independent experiments confirmed mitotic delay by non-phosphorylatable GFP-ZW10-S12A and abnormal anaphase by phospho-mimicking GFP-ZW10-S12D (Figure 5B and C; Supplementary Figure S6B and C). These observations are consistent with the role of ZW10 in spindle checkpoint regulation. We thus reason that dynamic phosphorylation of ZW10 is critical for accurate KT–MT attachment and spindle checkpoint silencing during mitosis.

Phosphorylation of ZW10 by PLK1 regulates the interaction between ZW10 with Zwint1

To elucidate mechanisms underlying the functional significance of dynamic phosphorylation of ZW10 in mitosis, we evaluated the influence of ZW10 phosphorylation on the ZW10–PLK1 interaction by performing co-IP assays. FLAG-PLK1 was precipitated with GFP-ZW10-WT and GFP-ZW10-S12A but much less with GFP-ZW10-S12D, suggesting a disruption of relevant protein–protein interactions by phosphorylation of ZW10 (Supplementary Figure S3D). Thus, the kinetochore localization of exogenously expressed GFP-tagged ZW10 proteins in HeLa cells depleted of endogenous ZW10 was examined. Both GFP-ZW10-WT and GFP-ZW10-S12A localized to the kinetochore in prophase cells and the signals were superimposed onto that of endogenous PLK1, while phospho-mimicking GFP-ZW10-S12D failed to localize to the kinetochore, where PLK1 remained normal (Figure 6A; Supplementary Figure S7A). Quantification of fluorescence intensities confirmed the significantly reduced kinetochore localization of GFP-ZW10-S12D and the unchanged kinetochore localization of PLK1 (Figure 6B; Supplementary Figure S7B). Western blotting analyses indicated that all three exogenous GFP-ZW10 variants were expressed at comparable levels to each other (Supplementary Figure S7C). However, they exhibited identical localization patterns in interphase cells (Supplementary Figure S7D and E). Moreover, when the protein level of ZW10 at the kinetochore was knocked down to be <20% of the control, that of PLK1 was barely changed (Figure 6C), suggesting that PLK1 localization to the kinetochore is independent of ZW10. Thus, we conclude that PLK1-mediated phosphorylation controls dynamic localization of ZW10 to the kinetochore in mitosis.

Since Zwint1 determines ZW10 localization to the kinetochore, which is essential for RZZ formation and Mad1/Mad2 recruitment to the fibrous corona (Wang et al., 2004; Kops et al., 2005), we also examined whether ZW10 phosphorylation affects its interaction with Zwint1 and other relevant proteins by anti-GFP IP with mitotic HeLa cell lysates. As shown in Figure 6D, GFP-ZW10-WT and GFP-ZW10-S12A pulled down comparable amounts of PLK1 and Zwint1 (lanes 4 and 5), while GFP-ZW10-S12D pulled down much less PLK1 and undetectable Zwint1 protein (lane 6), suggesting that phosphorylation of ZW10 disrupts its interaction with Zwint1 and hence its kinetochore localization. Coincidentally, GFP-ZW10-S12D failed to complex with Mad1/Mad2 (Figure 6, lane 6), accounting for the compromised spindle checkpoint observed in GFP-ZW10-S12D-expressing cells. These findings suggest that PLK1-mediated

Figure 4 (Continued) (C) Expression of GFP-ZW10 rescues ZW10 siRNA-elicited phenotypes. HeLa cells transfected with ZW10 siRNA along with siRNA-resistant GFP-ZW10 (si-R-GFP-ZW10) and mCherry-H2B were synchronized at 24 h post-transfection and then subjected to real-time imaging. Imaging began upon NEBD (0 min). The time is indicated in minutes. Merged images show chromosomes (red) and GFP-ZW10 (green). Scale bar, 10 μ m. (D) Quantitative analysis of the time intervals from NEBD to anaphase onset. $n = 50$ cells from three independent experiments for each group. Data are presented as mean \pm SD; two-sided t -test; **** $P < 0.0001$; ns, not significant. (E) Quantification of chromosome alignment and segregation defects in B and C. $n = 50$ cells for each group. Data are presented as mean \pm SD.

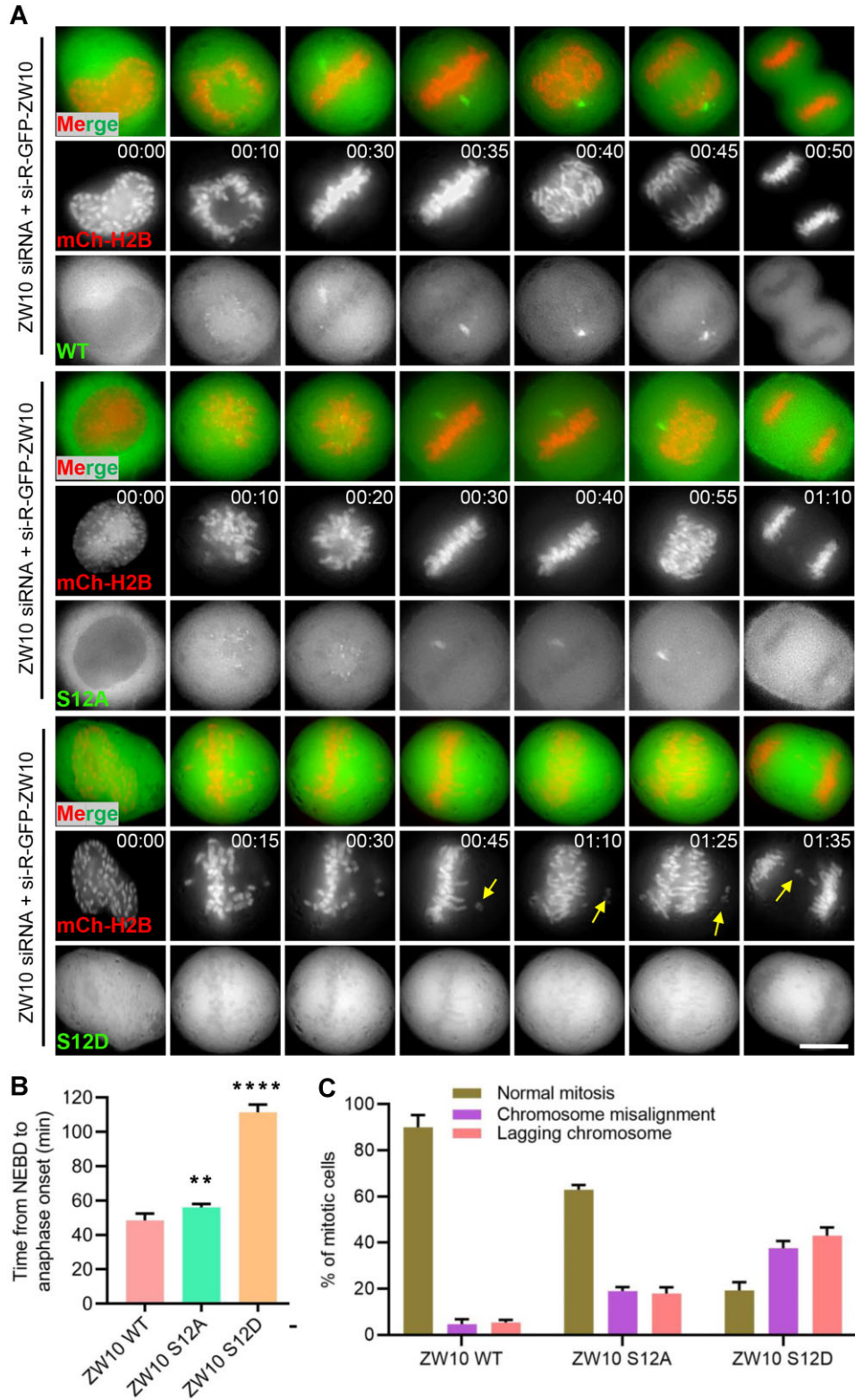


Figure 5 ZW10 phosphorylation promotes normal mitotic progression. **(A)** Real-time imaging of chromosome movements in HeLa cells co-transfected with mCherry-H2B and si-R-GFP-ZW10 (WT, S12A, or S12D) along with ZW10 siRNA. Imaging began upon NEBD (0 min). The time is indicated in minutes. Merged images show chromosomes (red) and GFP-ZW10 (green). Scale bar, 10 μ m. **(B)** Quantitative analysis of the time intervals from NEBD to anaphase onset. $n = 50$ cells from three independent experiments for each group. Data are presented as mean \pm SD; two-sided t -test; $^{**}P < 0.01$, $^{****}P < 0.0001$. **(C)** Quantification of chromosome alignment and segregation defects in **A**. $n = 50$ cells for each group. Data are presented as mean \pm SD.

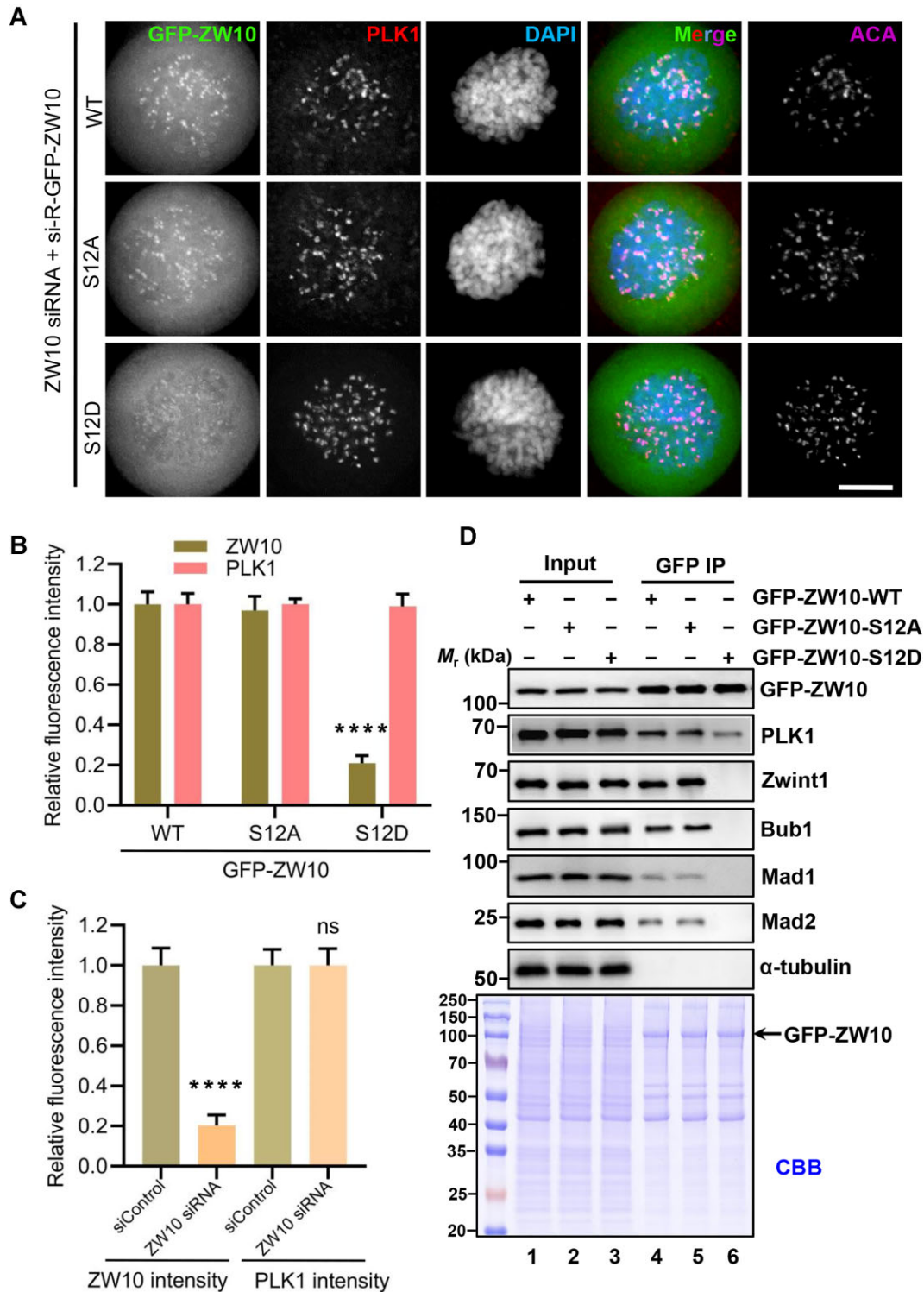


Figure 6 Phosphorylation of ZW10 by PLK1 weakens ZW10 localization to the kinetochore. **(A)** Phosphorylation of ZW10 by PLK1 attenuates the localization of ZW10 to kinetochores. HeLa cells were transfected with ZW10 siRNA along with si-R-GFP-ZW10 (WT, S12A, or S12D). At 48 h post-transfection, the cells were fixed and stained for PLK1 (red), centromere (ACA, magenta), and DNA (DAPI, blue). GFP-ZW10 and its mutants were visualized by direct GFP fluorescence. Scale bar, 10 μ m. **(B)** Quantification of ZW10 (WT, S12A, and S12D) and PLK1 intensities at the centromere/kinetochore. Note that the level of kinetochore-associated GFP-ZW10-S12D is much lower than that of GFP-ZW10-WT and GFP-ZW10-S12A. $n = 32$ mitotic cells from three independent experiments for each condition. Data are presented as mean \pm SD; two-sided t -test; **** $P < 0.0001$. **(C)** Quantification of ZW10 and PLK1 intensities at the centromere/kinetochore in ZW10-knockdown or control cells.

dynamic phosphorylation of ZW10 regulates spindle checkpoint satisfaction by modulating the interaction of ZW10 with Zwint1.

Discussion

In this study, we identified that ZW10, a subunit of RZZ, physically interacts with PLK1 both *in vitro* and *in vivo*. Our functional exploration demonstrated that ZW10 is a novel substrate of PLK1 and dynamic phosphorylation of ZW10 is required for correct KT–MT attachment, accurate chromosome segregation, and proper genomic stability (Figure 7). Interestingly, persistent phosphorylation of ZW10 attenuates its localization to the kinetochore, which results in chronic mitotic arrest and severe defects in spindle checkpoint satisfaction, such as premature anaphase with sister chromatid bridges. However, either suppression of ZW10 or expression of phosphorylation mutants did not affect the protein level and kinetochore localization of PLK1 during mitosis. Thus, the PLK1-elicited dynamic phosphorylation of ZW10 at Ser12 plays an important role in regulating dynamic localization of ZW10 to the kinetochore for spindle checkpoint signaling and satisfaction.

Our previous study showed that the interaction between ZW10 and Zwint1 is required for the spindle checkpoint machinery to ensure faithful chromosome segregation in mitosis (Wang et al., 2004). Checkpoint signaling requires the kinetochore localization of the Mad1–Mad2 complex, which depends on the RZZ complex. Zwint1 has been proposed to be the kinetochore receptor for RZZ and is critical for recruiting ZW10 to unattached kinetochores (Zhang et al., 2015). However, whether ZW10 is phosphorylated by any mitotic kinases has not been fully characterized. Here, we demonstrated that Ser12 of ZW10 is a cognate substrate of PLK1 and persistent phosphorylation at Ser12 perturbs the interaction of ZW10 with Zwint1. It has long been postulated that ZW10 functions as a linker between the core structural elements of the outer kinetochore and components that catalyze the generation of the mitotic checkpoint-derived ‘stop anaphase’ inhibitor (Kops et al., 2005). We reason that ZW10 phosphorylation by PLK1 is essential for spindle checkpoint satisfaction, as RZZ cooperates with Spindly to remove the spindle checkpoint complex from kinetochores to silence the checkpoint for anaphase onset. Notably, persistent phosphorylation of ZW10 at Ser12 did not completely abolish the SAC, suggesting that additional substrates/pathways may also participate in the checkpoint silencing process.

ZW10 possesses several important but context-dependent functions in mitosis, including accurate chromosome segregation, spindle checkpoint signaling, and spindle checkpoint

satisfaction. We reason that ZW10 is recruited to the kinetochore via Zwint1 for functional assembly of the spindle checkpoint complex, and ZW10 interaction with PLK1 and consequent phosphorylation of ZW10 at the kinetochore initiate spindle checkpoint satisfaction and silencing. PLK1 activity has been linked to both the stabilization (Elowe et al., 2007; Matsumura et al., 2007; Liu et al., 2012; Suijkerbuijk et al., 2012; Dumitru et al., 2017; Barbosa et al., 2020; Raisch et al., 2022) and destabilization (Ahonen et al., 2005; Foley et al., 2011; Salimian et al., 2011; Zhang et al., 2011; Hood et al., 2012; Moutinho-Santos et al., 2012; Paschal et al., 2012; Beck et al., 2013; Shao et al., 2015) of KT–MT attachments. However, the exact mechanism underlying its destabilizing action is still unclear. Interestingly, both the kinetochore localization and activity of PLK1 decline from early mitosis to metaphase (Ahonen et al., 2005; Conde et al., 2013). Furthermore, elevated PLK1 activity at the kinetochore has been linked to reduced KT–MT attachment stability during prometaphase (Foley et al., 2011; Zhang et al., 2011; Paschal et al., 2012; Beck et al., 2013), but the underlying molecular mechanisms were only slightly touched (Godek et al., 2015). Here, our data indicate that dynamic phosphorylation of ZW10 contributes to normal mitosis, i.e. accurate chromosome segregation, accurate KT–MT attachment, and correct SAC signaling, whereas persistent phosphorylation of ZW10 causes erroneous chromosome segregation and decreased stability of KT–MT attachment. In addition, persistent phosphorylation of ZW10 at Ser12 prevents the stable association of ZW10 with the kinetochore, which limits the activation and satisfaction of the spindle checkpoint (Figure 6A). Given that both phospho-mimicking and non-phosphorylatable ZW10 Ser12 mutants result in mitotic abnormalities but with distinct phenotypes, we performed the IP assay followed by mass spectrometric analyses to identify their respective binding partners (Supplementary Figure S3E and Tables S2 and S3). It will be exciting to delineate how these differential protein–protein interactions account for the observed distinctly different phenotypes. This can be achieved by using a proximity ligation approach with a cell synchronization protocol to capture these transient and low-affinity interactions (Liu et al., 2020).

Taken together, we propose that the phospho-regulation of ZW10 by PLK1 establishes faithful KT–MT attachment and spindle checkpoint satisfaction through temporal regulation of outer kinetochore protein recruitment at prometaphase and the removal of checkpoint components at metaphase. All the outer kinetochore proteins likely interact to orchestrate a functional kinetochore during chromosome segregation. The PLK1–ZW10 interaction established here is a core of this giant and dynamic complex, which orchestrates the robustness of the spindle

Figure 6 (Continued) Note that PLK1 localization to the centromere is independent of ZW10. $n = 32$ cells for each condition. Data are presented as mean \pm SD; two-sided t -test; **** $P < 0.0001$; ns, not significant. (D) GFP-tagged ZW10-WT, ZW10-S12A, and ZW10-S12D were expressed in 293T cells and purified with GFP-Trap Agarose beads. Subsequently, the beads were incubated with mitotic (100 ng/ml nocodazole, 16–18 h) HeLa cell lysates for 2 h, followed by extensive washes. The immunoprecipitates were resolved by SDS–PAGE and analyzed by western blotting using antibodies against GFP, PLK1, Zwint1, Bub1, Mad1, Mad2, and α -tubulin.

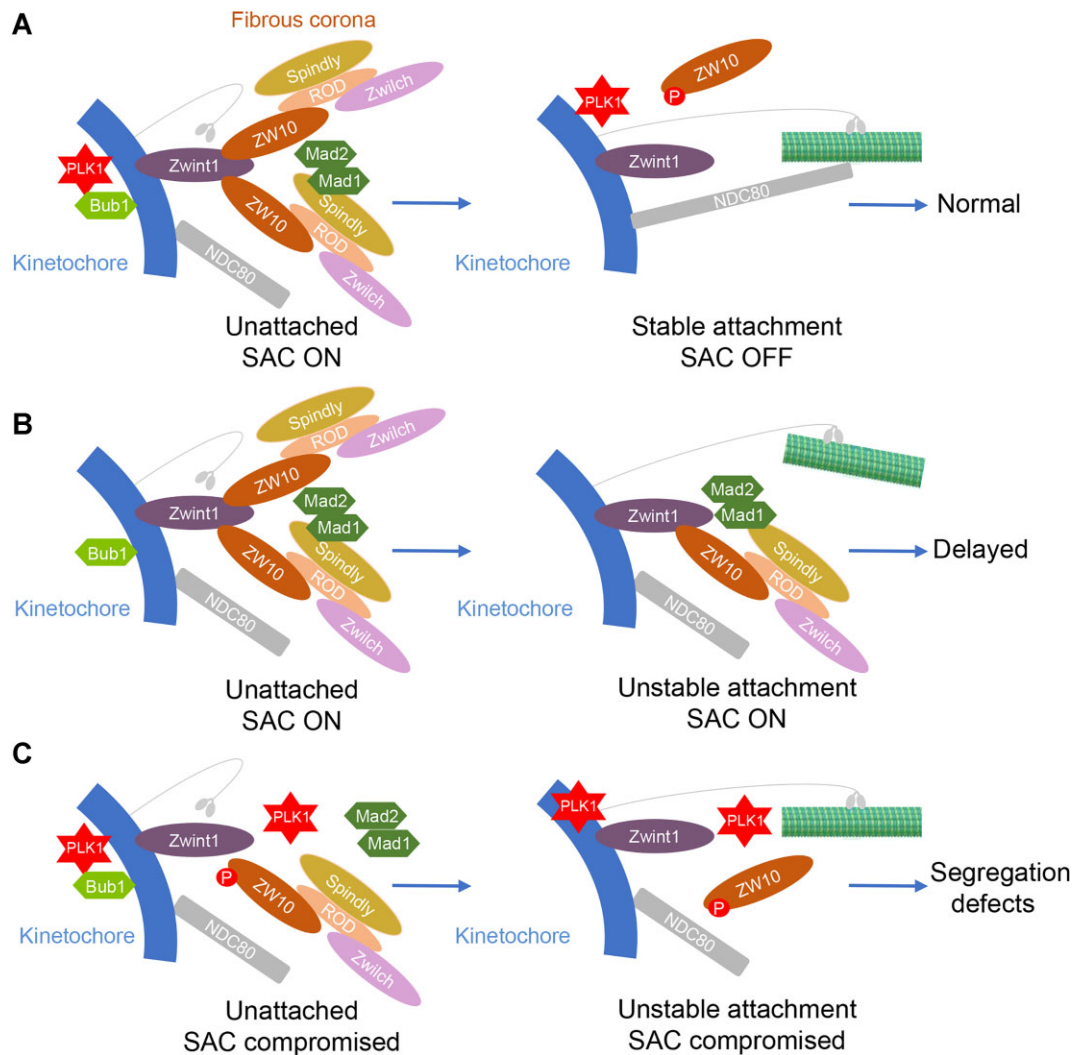


Figure 7 A proposed working model for the function of ZW10 phosphorylation by PLK1. For simplicity, the schematic shown here does not reflect the true size and conformation of the relevant proteins. **(A)** Under normal conditions, ZW10 is recruited by Zwint1 to the kinetochore to form the RZZ complex (ROD, Zwisch, and ZW10). RZZ coordinates with the NDC80 complex and motor proteins to regulate proper KT–MT attachment. RZZ also recruits checkpoint components and is thus required for functional assembly of the SAC complex. As kinetochores are captured by microtubules, PLK1 phosphorylates ZW10 to disrupt its interaction with Zwint1. RZZ likely works with Spindly to remove checkpoint complexes from the kinetochore. The checkpoint is then silenced, and stable KT–MT attachment is established for faithful chromosome segregation. **(B)** In contrast, if PLK1 cannot phosphorylate ZW10, accurate KT–MT attachment cannot be achieved in time, and the SAC silencing is also delayed, leading to incorrect chromosome capture and alignment. **(C)** However, if PLK1 is hyperactive or ZW10 is persistently phosphorylated, ZW10 cannot be efficiently recruited by Zwint1 to the kinetochore to form the RZZ complex. Thus, chromosome capture and the SAC were compromised, leading to erroneous chromosome segregation.

checkpoint for cell division quality control. Systemic analyses of spatiotemporal phosphorylation of ZW10 by mitotic kinases will shed light on spindle checkpoint satisfaction and chromosome stability control in mitosis.

Materials and methods

Plasmids, siRNAs, and transfection

The wild-type human ZW10 construct was generated by the recombination method, whereby both the ZW10 gene and the vectors pEGFP-N1, pEGFP-C1, pPET-22b, and pGEX-

6P-1 were amplified by polymerase chain reaction (PCR) and recombined according to the user’s manual of Vazyme C214. All site and deletion mutants of ZW10 were generated by a PCR-based mutagenesis approach. All the plasmids constructed in this study were sequenced for verification. ZW10 siRNA (5’-AAAUCCAGGAUAGAGAGUGAG-3’) (Wang et al., 2004) was synthesized by Dharmacon Research, Inc. PLK1 shRNA (5’-CCGGAGCTGCATCCTTGCAGGTCTCGAGACCTGCAAGGATGATGAGCTTTTTT-3’) targeting the 3’-UTR of the PLK1 gene was purchased from Sigma–Aldrich (TRCN0000011006). To knock

down the indicated proteins, HeLa cells were transfected with shRNA/siRNA oligonucleotides or control scramble oligonucleotides. The knockdown efficiency was judged by western blotting analysis. All the plasmids and shRNAs/siRNAs were transfected into cells using Lipofectamine 2000 or Lipofectamine 3000 (Invitrogen) according to the user's manual.

Cell culture, synchronization, and drug treatments

HEK293T, HeLa, and GFP-ZW10 stable HeLa Kyoto cells were routinely maintained in advanced Dulbecco's modified Eagle's medium (DMEM; Invitrogen) supplemented with 10% (v/v) fetal bovine serum (FBS; HyClone) plus 100 units/ml penicillin and 100 units/ml streptomycin (Gibco) at 37°C with 5% CO₂. To enrich mitotic cells, HeLa cells were treated with 2.5 mM thymidine (Invitrogen) for 16 h followed by release into fresh DMEM for the indicated periods (Mo et al., 2016). For IP of FLAG- and GFP-tagged proteins, HEK293T or HeLa cells were treated with nocodazole (100 ng/ml) for 16 h or not and then harvested for experiments. In some cases, the cells were treated with the indicated kinase inhibitor for another 1 h before the assays. The working concentrations of kinase inhibitors are as follows: PLK1 inhibitor BI2536, 100 nM; Cdk1 inhibitor RO-3306, 10 μM; Mps1 inhibitor reversine, 0.5 μM; and Aurora B inhibitor hesperidin, 0.1 μM. For some experiments, 20 μM MG132 was added to synchronize cells at metaphase.

Immunofluorescence microscopy, image processing, and quantification

For immunofluorescence, HeLa cells were seeded onto sterile acid-treated 12-mm coverslips in 24-well plates (Corning). Cells were transfected with the indicated siRNA and GFP-tagged plasmids using Oligofectamine Reagent or Lipofectamine 2000 (Invitrogen) according to the manufacturer's recommendations. The cells were then synchronized by thymidine release. Fixation and staining of cells were performed as described previously (Tian et al., 2018, 2022). Images were acquired using a Zeiss Axiovert 200 inverted microscope with AxioVision 3.0 software.

To quantify the fluorescence intensity of kinetochore proteins, images were collected using a DeltaVision deconvolution microscope (Applied Precision) built on an Olympus 1X71 inverted microscope base as described previously (Song et al., 2021). Quantification was conducted as previously described (Jiang et al., 2009; Huang et al., 2019). In brief, the pixel intensities of kinetochore pairs from each cell were measured, and background pixel intensities were subtracted. The pixel intensities were then normalized against ACA pixel values to account for any variations in staining or image acquisition. The values of the specifically treated cells were then plotted as a percentage of the average value obtained from the control cells.

Live cell imaging

For live cell imaging, HeLa cells were maintained in glass-bottom culture dishes (MatTek) and cultured at 37°C in CO₂-independent medium (Gibco) supplemented with 2 mM glutamine and 10% (v/v) FBS. Images of mitotic cells were acquired

at 3- or 5-min intervals using a DeltaVision deconvolution microscope (Applied Precision) with a 60× 1.42 NA objective. Images were projected using the softWoRx package and processed using ImageJ 1.51K software (Schneider et al., 2012).

Antibodies

Mouse anti-ZW10 (sc-81430, Santa Cruz Biotechnology), mouse anti-tubulin (#3873, Cell Signaling Technology), rabbit anti-GFP (#50430-2-AP, Proteintech), mouse anti-His tag (#2366, Cell Signaling Technology), mouse anti-FLAG (F3165, Sigma), rabbit anti-Cyclin B1 (#12231, Cell Signaling Technology), mouse anti-β-actin (GB15001, Servicebio), rabbit monoclonal anti-PLK1 (#4513, Cell Signaling Technology), mouse anti-Zwint1 (sc-271646, Santa Cruz Biotechnology), rabbit anti-phospho-PLK1 (Thr210) (#5472, Cell Signaling Technology), and anti-centromere antibodies (ACA; #HCT-0100, ImmunoVision) were obtained from commercial suppliers. Alexa 488-, Cy3-, or Cy5-conjugated secondary antibodies were purchased from Jackson ImmunoResearch and used at 1:500 for immunostaining. Horseradish peroxidase-conjugated anti-mouse or anti-rabbit antibodies (Jackson ImmunoResearch) and SuperSignal ECL (Pierce) were used for western blotting.

Recombinant protein expression and purification

The GST, GST-ZW10, GST-ZW10-S12A, His-PLK1, and His-MBP-CENP-U plasmids, respectively, were transformed into the *Escherichia coli* strain BL21(DE3), and protein expression was induced at a standard cell density (optical density ~0.6) with 0.2 mM isopropyl β-D-1-thiogalactopyranoside at 16°C for 20 h. Bacteria expressing His-PLK1 or His-MBP-CENP-U were lysed by sonication in Ni-NTA binding buffer (50 mM NaH₂PO₄, pH 8.0, 300 mM NaCl, and 10 mM imidazole), centrifuged, and incubated with Ni-NTA agarose (Qiagen) for 2 h at 4°C. The agarose was washed three times in Ni-NTA binding buffer supplemented with 30 mM imidazole and eluted with Ni-NTA binding buffer supplemented with 250 mM imidazole. Bacteria expressing recombinant GST, GST-ZW10, or GST-ZW10-S12A proteins were lysed by sonication in phosphate-buffered saline (PBS) supplemented with 0.1% Triton X-100, centrifuged, and incubated with Glutathione Sepharose 4B (GE Healthcare) for 2 h at 4°C. After three washes with lysis buffer, the GST, GST-ZW10, and GST-ZW10-S12A proteins were either eluted with 20 mM reduced glutathione or left on beads for further assays. All purification procedures were performed at 4°C, and a protease inhibitor cocktail (P8340, Sigma-Aldrich) was added to prevent protein degradation.

IP and pull-down assay

For the anti-FLAG IP assay, HEK293T or HeLa cells were transfected with the indicated plasmids, synchronized or not, collected, and lysed in lysis buffer (50 mM Tris-HCl, pH 7.4, 150 mM NaCl, and 1 mM EDTA) containing 0.1% Triton X-100 in the presence of mammalian protease inhibitor cocktail. After centrifugation, the cell lysates were incubated with anti-FLAG M2 beads (F2426, Sigma-Aldrich) at 4°C with

rotation for 2 h. The beads were then washed three times with lysis buffer containing 0.1% Triton X-100. The bound proteins were separated on a sodium dodecyl sulfate–polyacrylamide gel electrophoresis (SDS–PAGE) gel and transferred onto a nitrocellulose membrane for western blotting analysis. For anti-GFP IP, cells were lysed and processed similarly, except that GFP-Trap Agarose beads (GTA-20, ChromoTek) were used.

For endogenous IP, synchronized HeLa cells were harvested and lysed in lysis buffer (20 mM Tris–HCl, pH 7.5, 150 mM NaCl, 0.1% Triton X-100, and 2 mM EDTA) supplemented with protease inhibitor cocktail. After centrifugation and pre-clearing with protein A/G resin, the lysates were incubated with ZW10 antibody at 4°C for 24 h with gentle rotation. Protein A/G resin was then added, incubated for another 6 h, and spun down. The immunoprecipitates were washed three times with lysis buffer before being resolved by SDS–PAGE, transferred onto a nitrocellulose membrane, and immunoblotted with the indicated antibodies (Wang et al., 2021).

The pull-down assay with purified GST-ZW10 and His-PLK1 was performed as previously described (Xu et al., 2021). Purified GST-ZW10 on glutathione beads was used as an affinity matrix to absorb His-tagged PLK1 in PBS containing 0.1% Triton X-100 and 1 mM phenylmethylsulfonyl fluoride for 3 h at 4°C. The beads were washed three times with PBS plus 0.1% Triton X-100 and once with PBS only and then boiled for 5 min in SDS–PAGE sample buffer. Proteins were resolved by SDS–PAGE, followed by CBB staining and western blotting.

In vitro phosphorylation assay

In vitro phosphorylation assays were carried out as described previously (Yu et al., 2020). PLK1 kinase was purchased from Cell Signaling Technology. The kinase reactions were performed in 40 μ l of 1 \times kinase buffer (25 mM HEPES, pH 7.2, 50 mM NaCl, 2 mM EGTA, 5 mM MgSO₄, 1 mM 1,4-dithiothreitol (DTT), and 0.01% Brij35) containing 200 ng of PLK1 kinase, 3–5 μ g of GST- or MBP-tagged proteins, and 500 μ M ATP. The mixtures were incubated at 30°C for 30 min, and the reactions were stopped by the addition of SDS–PAGE sample buffer. Proteins were then separated by Phos-tag SDS–PAGE and detected using the indicated antibodies.

Mass spectrometric sample preparation and analyses

The sample from IP was reduced with 10 mM DTT in 50 mM ammonium bicarbonate at 56°C for 30 min and then alkylated with 30 mM iodoacetamide for 30 min in the dark. Then, 1 μ g trypsin (Promega, V5111) was added to the sample for overnight digestion at 37°C. The peptides were desalted and analyzed with a Thermo Scientific Orbitrap Exploris 480 mass spectrometer. The raw file was analyzed with PD2.5. The human database from UniProt (proteome ID: UP000005640) was used for searching. Phosphorylation (S/T, +79.9663 Da) and oxidation (M, +15.9949 Da) modifications were included as variable modifications. Carbamidomethyl (C, +57.0215 Da) was set as a fixed modification.

Statistics

All statistics are described in figure legends. The two-sided unpaired Student's *t*-test was applied for experimental comparisons using GraphPad Prism 7, and *P* < 0.05 was considered significant.

Supplementary material

Supplementary material is available at *Journal of Molecular Cell Biology* online.

Acknowledgements

We thank all the members of our laboratory for insightful discussion and suggestions.

Funding

This work was supported by grants from the Ministry of Science and Technology of China and the National Natural Science Foundation of China (2022YFA1303100, 32090040, 92254302, 2022YFA0806800, 91854203, 31621002, 2017YFA0503600, 21922706, and 92153302 to X.L.; 92053104 to X.G.), the Plans for Major Provincial Science & Technology Projects of Anhui Province (202303a0702003 to X.L.), the Ministry of Education (IRT_17R102 to X.L.), and the Fundamental Research Funds for the Central Universities (KB9100000007 and KB9100000013 to X.L.). The funders had no role in the study design, data collection and analysis, decision to publish, or preparation of the manuscript.

Conflict of interest: none declared.

Author contributions: X.Y. conceived the project. S.F.B., Z.D., F.X., F.Y., X.L., L.Z., and X.G. performed the experiments and analyzed the data. S.F.B., Z.D., X.G., L.Z., and X.Y. wrote the manuscript. S.F.B., Z.D., F.X., X.L., X.G., L.Z., and X.Y. reviewed the manuscript. All the authors have commented on and approved the manuscript.

References

- Ahonen, L.J., Kallio, M.J., Daum, J.R., et al. (2005). Polo-like kinase 1 creates the tension-sensing 3F3/2 phosphoepitope and modulates the association of spindle-checkpoint proteins at kinetochores. *Curr. Biol.* 15, 1078–1089.
- Amin, M.A., McKenney, R.J., and Varma, D. (2018). Antagonism between the dynein and Ndc80 complexes at kinetochores controls the stability of kinetochore–microtubule attachments during mitosis. *J. Biol. Chem.* 293, 5755–5765.
- Archambault, V., and Glover, D.M. (2009). Polo-like kinases: conservation and divergence in their functions and regulation. *Nat. Rev. Mol. Cell Biol.* 10, 265–275.
- Barbosa, J., Martins, T., Bange, T., et al. (2020). Polo regulates Spindly to prevent premature stabilization of kinetochore–microtubule attachments. *EMBO J.* 39, e100789.
- Barisic, M., and Geley, S. (2011). Spindly switch controls anaphase: Spindly and RZZ functions in chromosome attachment and mitotic checkpoint control. *Cell Cycle* 10, 449–456.

- Basto, R., Gomes, R., and Kress, R.E. (2000). Rough deal and Zw10 are required for the metaphase checkpoint in *Drosophila*. *Nat. Cell Biol.* 2, 939–943.
- Beck, J., Maerki, S., Posch, M., et al. (2013). Ubiquitylation-dependent localization of PLK1 in mitosis. *Nat. Cell Biol.* 15, 430–439.
- Buffin, E., Lefebvre, C., Huang, J., et al. (2005). Recruitment of Mad2 to the kinetochore requires the Rod/Zw10 complex. *Curr. Biol.* 15, 856–861.
- Chu, Y., Yao, P.Y., Wang, W., et al. (2011). Aurora B kinase activation requires survivin priming phosphorylation by PLK1. *J. Mol. Cell Biol.* 3, 260–267.
- Cleveland, D.W., Mao, Y., and Sullivan, K.F. (2003). Centromeres and kinetochores: from epigenetics to mitotic checkpoint signaling. *Cell* 112, 407–421.
- Conde, C., Osswald, M., Barbosa, J., et al. (2013). *Drosophila* Polo regulates the spindle assembly checkpoint through Mps1-dependent BubR1 phosphorylation. *EMBO J.* 32, 1761–1777.
- Ding, X., Deng, H., Wang, D., et al. (2010). Phospho-regulated ACAP4–Ezrin interaction is essential for histamine-stimulated parietal cell secretion. *J. Biol. Chem.* 285, 18769–18780.
- Dumitru, A.M.G., Rusin, S.F., Clark, A.E.M., et al. (2017). Cyclin A/Cdk1 modulates Plk1 activity in prometaphase to regulate kinetochore–microtubule attachment stability. *eLife* 6, e29303.
- Elia, A.E., Cantley, L.C., and Yaffe, M.B. (2003a). Proteomic screen finds pSer/pThr-binding domain localizing Plk1 to mitotic substrates. *Science* 299, 1228–1231.
- Elia, A.E., Rellos, P., Haire, L.F., et al. (2003b). The molecular basis for phosphodependent substrate targeting and regulation of Plks by the Polo-box domain. *Cell* 115, 83–95.
- Elowe, S., Hummer, S., Uldschmid, A., et al. (2007). Tension-sensitive Plk1 phosphorylation on BubR1 regulates the stability of kinetochore–microtubule interactions. *Genes Dev.* 21, 2205–2219.
- Fang, Z., Miao, Y., Ding, X., et al. (2006). Proteomic identification and functional characterization of a novel ARF6 GTPase-activating protein ACAP4. *Mol. Cell. Proteomics* 5, 1437–1449.
- Foley, E.A., Maldonado, M., and Kapoor, T.M. (2011). Formation of stable attachments between kinetochores and microtubules depends on the B56-PP2A phosphatase. *Nat. Cell Biol.* 13, 1265–1271.
- Gimenez-Abian, J.F., Sumara, I., Hirota, T., et al. (2004). Regulation of sister chromatid cohesion between chromosome arms. *Curr. Biol.* 14, 1187–1193.
- Godek, K.M., Kabeche, L., and Compton, D.A. (2015). Regulation of kinetochore–microtubule attachments through homeostatic control during mitosis. *Nat. Rev. Mol. Cell Biol.* 16, 57–64.
- Golsteyn, R.M., Mundt, K.E., Fry, A.M., et al. (1995). Cell cycle regulation of the activity and subcellular localization of Plk1, a human protein kinase implicated in mitotic spindle function. *J. Cell Biol.* 129, 1617–1628.
- Hanisch, A., Wehner, A., Nigg, E.A., et al. (2006). Different Plk1 functions show distinct dependencies on polo-box domain-mediated targeting. *Mol. Biol. Cell* 17, 448–459.
- Hirose, H., Arasaki, K., Dohmae, N., et al. (2004). Implication of ZW10 in membrane trafficking between the endoplasmic reticulum and Golgi. *EMBO J.* 23, 1267–1278.
- Hood, E.A., Kettenbach, A.N., Gerber, S.A., et al. (2012). Plk1 regulates the kinesin-13 protein Kif2b to promote faithful chromosome segregation. *Mol. Biol. Cell* 23, 2264–2274.
- Hua, S., Wang, Z., Jiang, K., et al. (2011). CENP-U cooperates with Hec1 to orchestrate kinetochore–microtubule attachment. *J. Biol. Chem.* 286, 1627–1638.
- Huang, Y., Lin, L., Liu, X., et al. (2019). BubR1 phosphorylates CENP-E as a switch enabling the transition from lateral association to end-on capture of spindle microtubules. *Cell Res.* 29, 562–578.
- Jiang, K., Wang, J., Liu, J., et al. (2009). TIP150 interacts with and targets MCAK at the microtubule plus ends. *EMBO Rep.* 10, 857–865.
- Karess, R. (2005). Rod–Zw10–Zwilch: a key player in the spindle checkpoint. *Trends Cell Biol.* 15, 386–392.
- Kops, G.J., Kim, Y., Weaver, B.A., et al. (2005). ZW10 links mitotic checkpoint signaling to the structural kinetochore. *J. Cell Biol.* 169, 49–60.
- Lampson, M.A., and Cheeseman, I.M. (2011). Sensing centromere tension: Aurora B and the regulation of kinetochore function. *Trends Cell Biol.* 21, 133–140.
- Lampson, M.A., and Kapoor, T.M. (2005). The human mitotic checkpoint protein BubR1 regulates chromosome–spindle attachments. *Nat. Cell Biol.* 7, 93–98.
- Lenart, P., Petronczki, M., Steegmaier, M., et al. (2007). The small-molecule inhibitor BI 2536 reveals novel insights into mitotic roles of polo-like kinase 1. *Curr. Biol.* 17, 304–315.
- Liu, D., Davydenko, O., and Lampson, M.A. (2012). Polo-like kinase-1 regulates kinetochore–microtubule dynamics and spindle checkpoint silencing. *J. Cell Biol.* 198, 491–499.
- Liu, D., Vader, G., Vromans, M.J., et al. (2009). Sensing chromosome bi-orientation by spatial separation of Aurora B kinase from kinetochore substrates. *Science* 323, 1350–1353.
- Liu, X., Liu, X., Wang, H., et al. (2020). Phase separation drives decision making in cell division. *J. Biol. Chem.* 295, 13419–13431.
- Matsumura, S., Toyoshima, F., and Nishida, E. (2007). Polo-like kinase 1 facilitates chromosome alignment during prometaphase through BubR1. *J. Biol. Chem.* 282, 15217–15227.
- Mo, F., Zhuang, X., Liu, X., et al. (2016). Acetylation of Aurora B by TIP60 ensures accurate chromosomal segregation. *Nat. Chem. Biol.* 12, 226–232.
- Moutinho-Santos, T., Conde, C., and Sunkel, C.E. (2012). POLO ensures chromosome bi-orientation by preventing and correcting erroneous chromosome–spindle attachments. *J. Cell Sci.* 125, 576–583.
- Paschal, C.R., Maciejowski, J., and Jallepalli, P.V. (2012). A stringent requirement for Plk1 T210 phosphorylation during K-fiber assembly and chromosome congression. *Chromosoma* 121, 565–572.
- Raisch, T., Ciossani, G., d' Amico, E., et al. (2022). Structure of the RZZ complex and molecular basis of Spindly-driven corona assembly at human kinetochores. *EMBO J.* 41, e110411.
- Salimian, K.J., Ballister, E.R., Smoak, E.M., et al. (2011). Feedback control in sensing chromosome biorientation by the Aurora B kinase. *Curr. Biol.* 21, 1158–1165.
- Scaerou, F., Starr, D.A., Piano, F., et al. (2001). The ZW10 and Rough Deal checkpoint proteins function together in a large, evolutionarily conserved complex targeted to the kinetochore. *J. Cell Sci.* 114, 3103–3114.
- Schmucker, S., and Sumara, I. (2014). Molecular dynamics of PLK1 during mitosis. *Mol. Cell. Oncol.* 1, e954507.
- Schneider, C.A., Rasband, W.S., and Eliceiri, K.W. (2012). NIH Image to ImageJ: 25 years of image analysis. *Nat. Methods* 9, 671–675.
- Shao, H., Huang, Y., Zhang, L., et al. (2015). Spatiotemporal dynamics of Aurora B–PLK1–MCAK signaling axis orchestrates kinetochore bi-orientation and faithful chromosome segregation. *Sci. Rep.* 5, 12204.
- Singh, P., Pesenti, M.E., Maffini, S., et al. (2021). BUB1 and CENP-U, primed by CDK1, are the main PLK1 kinetochore receptors in mitosis. *Mol. Cell* 81, 67–87.e69.
- Song, X., Yang, F., Liu, X., et al. (2021). Dynamic crotonylation of EB1 by TIP60 ensures accurate spindle positioning in mitosis. *Nat. Chem. Biol.* 17, 1314–1323.
- Suijkerbuijk, S.J., Vleugel, M., Teixeira, A., et al. (2012). Integration of kinase and phosphatase activities by BUBR1 ensures formation of stable kinetochore–microtubule attachments. *Dev. Cell* 23, 745–755.
- Sumara, I., Giménez-Abián, J.F., Gerlich, D., et al. (2004). Roles of polo-like kinase 1 in the assembly of functional mitotic spindles. *Curr. Biol.* 14, 1712–1722.
- Takaki, T., Trenz, K., Costanzo, V., et al. (2008). Polo-like kinase 1 reaches beyond mitosis–cytokinesis, DNA damage response, and development. *Curr. Opin. Cell Biol.* 20, 650–660.
- Tian, T., Chen, L., Dou, Z., et al. (2022). Structural insights into human CCAN complex assembled onto DNA. *Nature* 8, 90.
- Tian, T., Li, X., Liu, Y., et al. (2018). Molecular basis for CENP-N recognition of CENP-A nucleosome on the human kinetochore. *Cell Res.* 28, 374–378.

- Wang, H., Hu, X., Ding, X., et al. (2004). Human Zwint-1 specifies localization of Zeste White 10 to kinetochores and is essential for mitotic checkpoint signaling. *J. Biol. Chem.* 279, 54590–54598.
- Wang, X., Wang, W., Wang, X., et al. (2021). The septin complex links the catenin complex to the actin cytoskeleton for establishing epithelial cell polarity. *J. Mol. Cell Biol.* 13, 395–408.
- Williams, B.C., Gatti, M., and Goldberg, M.L. (1996). Bipolar spindle attachments affect redistributions of ZW10, a *Drosophila* centromere/kinetochore component required for accurate chromosome segregation. *J. Cell Biol.* 134, 1127–1140.
- Williams, B.C., Li, Z., Liu, S., et al. (2003). Zwilch, a new component of the ZW10/ROD complex required for kinetochore functions. *Mol. Biol. Cell* 14, 1379–1391.
- Xu, L., Ali, M., Duan, W., et al. (2021). Feedback control of PLK1 by Apolo1 ensures accurate chromosome segregation. *Cell Rep.* 36, 109343.
- Yu, R., Wu, H., Ismail, H., et al. (2020). Methylation of PLK1 by SET7/9 ensures accurate kinetochore–microtubule dynamics. *J. Mol. Cell Biol.* 12, 462–476.
- Yuan, K., Hu, H., Guo, Z., et al. (2007). Phospho-regulation of HsCDC14A by polo-like kinase 1 is essential for mitotic progression. *J. Biol. Chem.* 282, 27414–27423.
- Zhang, G., Lischetti, T., Hayward, D.G., et al. (2015). Distinct domains in Bub1 localize RZZ and BubR1 to kinetochores to regulate the checkpoint. *Nat. Commun.* 6, 7162.
- Zhang, L., Shao, H., Huang, Y., et al. (2011). PLK1 phosphorylates mitotic centromere-associated kinesin and promotes its depolymerase activity. *J. Biol. Chem.* 286, 3033–3046.
- Zitouni, S., Nabais, C., Jana, S.C., et al. (2014). Polo-like kinases: structural variations lead to multiple functions. *Nat. Rev. Mol. Cell Biol.* 15, 433–452.

Received September 3, 2023. Revised November 9, 2023. Accepted February 23, 2024.

© The Author(s) (2024). Published by Oxford University Press on behalf of *Journal of Molecular Cell Biology*, CEMCS, CAS.

This is an Open Access article distributed under the terms of the Creative Commons Attribution-NonCommercial License (<https://creativecommons.org/licenses/by-nc/4.0/>), which permits non-commercial re-use, distribution, and reproduction in any medium, provided the original work is properly cited. For commercial re-use, please contact journals.permissions@oup.com